Age-dependent tissue-specific exposure of cell phone users

2010 Phys. Med. Biol. 55 1767

(http://iopscience.iop.org/0031-9155/55/7/001)

IOP PUBLISHING PHYSICS IN MEDICINE AND BIOLOGY

Phys. Med. Biol. **55** (2010) 1767–1783 doi:10.1088/0031-9155/55/7/001

Age-dependent tissue-specific exposure of cell phone users

Andreas Christ[1], Marie-Christine Gosselin[1], Maria Christopoulou[2], Sven Kühn[1,3] and Niels Kuster[1,3]

[1] Foundation for Research on Information Technologies in Society (IT'IS), Zeughausstr. 43, 8004 Zürich, Switzerland
[2] National Technical University of Athens, School of Electrical and Computer Engineering, 9 Iroon Polytechniou Str., 15780 Athens, Greece
[3] Swiss Federal Institute of Technology (ETHZ), Rämistr. 101, 8092 Zürich, Switzerland

E-mail: christ@itis.ethz.ch

Received 18 August 2009, in final form 6 January 2010
Published 5 March 2010
Online at stacks.iop.org/PMB/55/1767

Abstract

The peak spatial specific absorption rate (SAR) assessed with the standardized specific anthropometric mannequin head phantom has been shown to yield a conservative exposure estimate for both adults and children using mobile phones. There are, however, questions remaining concerning the impact of age-dependent dielectric tissue properties and age-dependent proportions of the skull, face and ear on the global and local absorption, in particular in the brain tissues. In this study, we compare the absorption in various parts of the cortex for different magnetic resonance imaging-based head phantoms of adults and children exposed to different models of mobile phones. The results show that the locally induced fields in children can be significantly higher (>3 dB) in subregions of the brain (cortex, hippocampus and hypothalamus) and the eye due to the closer proximity of the phone to these tissues. The increase is even larger for bone marrow (>10 dB) as a result of its significantly high conductivity. Tissues such as the pineal gland show no increase since their distances to the phone are not a function of age. This study, however, confirms previous findings saying that there are no age-dependent changes of the peak spatial SAR when averaged over the entire head.

1. Introduction

Potential differences between adults and children in exposure to cell phone radiation have been the subject of ongoing debate regarding both dosimetric aspects and the possibly greater sensitivity of children, in particular their developing brain. Whereas recent interpretations of epidemiological studies indicating an increased risk for glioma and acoustic neuroma (Khurana

et al 2009) are being controversially discussed within the scientific community (Khurana *et al* 2008, Kundi 2009), the correlation of different ailments of the central nervous system (CNS), such as Alzheimer's and migraine or vertigo, with electromagnetic field exposure has gained additional research interest among epidemiologists (Huss *et al* 2009, Schüz *et al* 2009).

During the last decade, the dosimetric analysis of cell phone exposure focused on testing the compliance of mobile phones with basic restrictions, i.e. the peak spatial average specific absorption rate (psSAR) as defined by ICNIRP (1998), IEEE (2005)[4]. Anatomical head models of adults and children were used to assess the psSAR in the human head for different phones, the results of which were compared to those assessed for the specific anthropometric mannequin (SAM). The SAM was proposed by the standards (CENELEC 2001, IEEE 2003, IEC 2005) for demonstrating cell phone compliance with safety limits. A large number of studies evaluated the psSAR in the SAM phantom with respect to anatomical head models, and all reviews of these studies came to the conclusion that the psSAR assessed with the SAM is a conservative measure for the exposure of both adults and children (Martens 2005, Wiart *et al* 2005, Christ and Kuster 2005) and that variations in psSAR among different models can be attributed to individual anatomical differences but not to age-dependent changes in head size (Kainz *et al* 2005). Remaining open issues, however, concern the effect of age-dependent changes of the dielectric tissue parameters on the psSAR as well as systematic differences in the local exposure, in particular of the cortex. Regarding the incomplete knowledge of these aspects, the higher lifetime exposure and the developing bodies of children, the World Health Organization recommends the development of a precautionary approach (Kheifets *et al* 2005).

Age-dependent changes of the loss of tissue conductivity have been repeatedly reported in the past (Thurai *et al* 1984, 1985, Peyman *et al* 2001, Gabriel 2005, Schmid and Überbacher 2005), but the available data did not suffice for a comprehensive analysis. A systematic evaluation of the age-dependent changes of the dielectric properties of a large number of different tissues has only been published very recently (Peyman *et al* 2009). Moreover, differences in the exposure of particular brain regions due to growth-dependent changes of the proportions of the head and the face have not been evaluated. A large number of numerical studies on absorption in the heads of children use scaled models of adults. Since this approach can lead to large uncertainties with respect to the local exposure of tissues and therefore to the interpretation of the findings, it has repeatedly been discouraged (Bit-Babik *et al* 2005, Wiart *et al* 2008). Several head models of children were recently developed based on magnetic resonance imaging (MRI), and systematic differences in the exposure of the peripheral brain regions of adults and children were observed (Wiart *et al* 2008).

This study aims at clarification of the remaining open questions discussed above using anatomically correct models of adults and children. In detail, its objectives are

- assessment of differences of the psSAR considering age-dependent changes of the anatomy of the head and dielectric tissue properties, and
- assessment of the differences of the local exposure of the cortex and other distinguished brain regions.

2. Methods and models

2.1. Anatomical head models

Anatomically correct high-resolution models of the heads of two adults and four children (three to eleven years of age) were used in this study (figure 1), three of which are part of

[4] The psSAR is the maximum absorbed energy anywhere in the body and, irrespective of the tissue composition, averaged over any 1 g (IEEE 2005) or 10 g (ICNIRP 1998) of tissue.

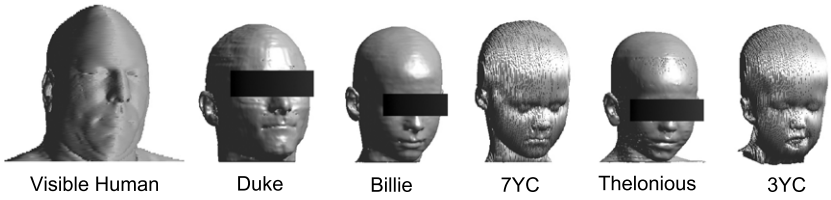

Figure 1. Anatomical head models (from left to right): 38-year-old male adult, 34-year-old male adult, 11-year-old girl, 7-year-old child, 6-year-old boy, 3-year-old child.

the 'Virtual Family'. These models provide significantly improved accuracy with respect to their spatial resolution and their level of detail (Christ *et al* 2010). Their characteristics are as follows.

- *Visible human.* The model is based on cryosection images of a 38-year-old adult male (Ackerman 1998). The segmentation distinguishes approximately 40 tissue types. They are represented in a 2.5-dimensional 'compound format' that maintains the original outlines of the image slices in the cross section of the body and uses a staircased representation with 1 mm step size along the body axis (Christ *et al* 2005).
- *Duke.* The 34-year-old male adult model of the 'Virtual Family' was developed from magnetic resonance images with a resolution of $0.5 \times 0.5 \times 1.0$ mm^3 in the head region. It consists of approximately 40 different organs and tissues that were reconstructed as triangular surface meshes (Christ *et al* 2010).
- *Billie.* The head model of an 11-year-old girl is part of the 'Virtual Family'. Technically it corresponds to the model Duke (see above).
- *7YC.* The model of a seven-year-old child is based on MRI scans (Schönborn *et al* 1998). The images were taken in sagittal orientation at a distance of 1.1 mm. It consists of approximately 20 different tissues and organs that are represented in the 'compound format' mentioned above.
- *Thelonious.* The head model of a six-year-old boy is part of the 'Virtual Family'. Technically it corresponds to the model Duke (see above).
- *3YC.* The model of a three-year-old child corresponds technically to the model 7YC.

For analysis of the exposure of the inner brain regions, the hypothalami, the hippocampi and the pineal glands were resegmented in the images of the models 3YC, Thelonious, 7YC, Billie and Visible Human. Figure 2 shows these brain regions in the head of the model Thelonious. The dielectric parameters of gray matter were used for the hypothalamus, the hippocampus and the pineal gland (section 2.2). The 'Virtual Family' models are available for research purposes at www.itis.ethz.ch[5].

2.2. *Age-dependent tissue parameters*

Most data on the dielectric properties of tissue used in numerical dosimetry were obtained from measurements of different mammals, such as pigs, sheep or rabbits. Several studies show that the differences of these values to adult human tissue are within the variations of the dielectric properties among different species of fully grown animals (Pethig 1987, Gabriel *et al* 1996a, Stauffer *et al* 2003). Based on these measurements, a parametric model using four Cole–Cole dispersion terms has been proposed by Gabriel *et al* (1996b). This model has

[5] The order form for the models is available under http://www.itis.ethz.ch/index/index_humanmodels.html. A shipping and handling fee applies.

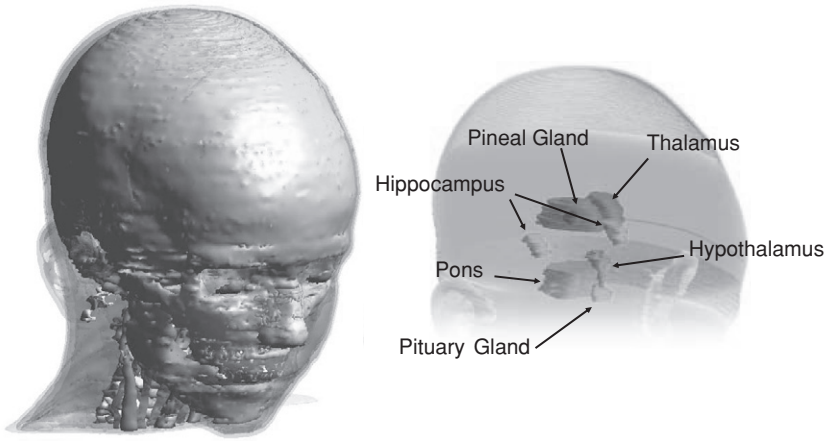

Figure 2. Segmented brain regions of the model of the six-year-old boy (Thelonious).

been used extensively in numerical dosimetry of the human body and of animals by many different research groups (Hand 2008).

With respect to their dielectric properties, biological tissues can be roughly classified by their water content (Gabriel *et al* 1996a). Typical tissues with low water content are e.g. fat, breast tissue or bone. In the frequency range of interest of this study, their permittivities ϵ_r range from approximately 5 to 20 and their conductivities from approximately 0.05 S m^{-1} to 0.3 S m^{-1}. Tissues with high water content can reach values of approximately 60 for their relative permittivity and up to 2 S m^{-1} for their conductivity.

Until recently, the available data on age-dependent changes of the tissue dielectrics (Thurai *et al* 1984, 1985, Peyman *et al* 2001, Gabriel 2005, Schmid and Überbacher 2005) were not sufficient for a comprehensive analysis, which has already been mentioned in section 1. In order to overcome these limitations Wang *et al* (2006) suggested to use the total body water as a proxy to model the impact of its age-dependent changes on the dielectric properties of those tissues which are relevant for the SAR calculation in the head. The parameters of rat tissues of differently aged samples are used to extrapolate permittivity and conductivity. Whereas the model predicts age-dependent changes of high water content tissues with satisfactory accuracy, larger deviations from the experimental results are reported for the skull (low water content tissue). Applying the parameters of the model on the calculation of the psSAR does not reveal any systematic changes within the assumed age groups.

A recent study reports on the dielectric tissue parameters of pigs with body weight ranging from 10 kg to 250 kg corresponding approximately to ages of 35, 100 and 600 days (Peyman *et al* 2009). Table 1 shows the dielectric parameters of those tissues that are most relevant for the assessment of absorption in the head at the frequencies 900 MHz and 1800 MHz[6]. For comparison, the values of the Cole–Cole model (Gabriel *et al* 1996b, IFAC 2007) are given as well. Tissues with high water content only show small changes with age and are in generally good agreement with the Cole–Cole model. However, significant differences at young age can be observed for tissues that have a low water content i.e. the skull, fat and bone marrow. These tissues show a significantly higher permittivity and conductivity for the younger age groups. With increasing age, they tend toward the values of the Cole–Cole model.

[6] Both trends and absolute values of gray and white matter are in good agreement with the measurement results for the bovine brain reported in Schmid and Überbacher (2005).

Table 1. Age dependent properties of the tissues in the head (Peyman *et al* 2009) in comparison to the Cole–Cole model.

		ϵ_r				σ in S m^{-1}			
	Frequency	Cole–Cole	250 kg	50 kg	10 kg	Cole–Cole	250 kg	50 kg	10 kg
Gray Matter	900 MHz	52.7	49.9	50.9	51.7	0.94	1.00	1.00	0.98
White Matter		38.9	28.6	34.0	39.8	0.59	0.48	0.59	0.67
Bone Marrow		11.3	5.7	14.0	39.5	0.22	0.05	0.23	0.77
Skull		20.8	18.8	34.3	41.1	0.34	0.26	0.65	0.75
Skin		41.4	36.8	44.2	45.5	0.87	0.62	0.78	0.80
Fat		5.46	5.7	12.8	14.3	0.05	0.06	0.21	0.23
Gray Matter	1800 MHz	50.1	48.1	49.2	49.7	1.39	1.34	1.33	1.30
White Matter		37.0	27.4	32.7	38.2	0.91	0.68	0.82	0.94
Bone Marrow		10.7	5.6	13.5	37.9	0.35	0.08	0.34	1.09
Skull		19.3	17.8	32.6	39.2	0.59	0.44	0.95	1.11
Skin		38.9	34.9	42.1	43.2	1.18	0.93	1.16	1.17
Fat		5.3	5.6	12.6	14.0	0.08	0.10	0.30	0.34

For the dosimetric simulations (section 3), the four different sets of tissue parameters listed in table 1 were used. Since they do not cover all of the head tissues of the models, they were complemented by the Cole–Cole model. Nevertheless, the parameters given in table 1 account for about 70% of the tissue masses of the head models. The only tissue with a major contribution to the mass of the head for which no age-dependent parameters are available is muscle tissue (approximately 20% of the mass of the head and the neck). Among the age-dependent parameters reported in Peyman *et al* (2009), tongue tissue is closest to muscle with respect to its dielectric characteristics. The changes of the dielectric parameters of tongue tissue with age are comparatively small (<3% over the reported age range). Therefore, Cole–Cole parameters without age-dependent changes are used for muscle tissue for all simulations. The Cole–Cole model was always used for the tissues of the eye, since the only dielectric properties of the lens show certain changes with age, whereas the predominant part (>95%) of its volume (vitreous body, cornea) does not show any changes (Schmid and Überbacher 2005). Gray matter with age-dependent dielectrics was used for the subregions of the brain shown in figure 2.

The direct correlation of the ages at which the dielectric properties of the tissue samples were taken to human age is not possible. Nevertheless, the available data can be assumed to cover the entire range of changes from newborn to fully grown. Even if the absolute values may not be applicable to human tissue, it should be considered that the dielectric properties of animal tissue have been shown to be in generally good agreement with those of human tissue. Therefore, the application of these parameters will identify trends as a function of age and indicate the order of magnitude of the changes in exposure that can be expected. In order to separate the impact of individual anatomical features of the head models (section 2.1) on the exposure, all models are evaluated with all four sets of tissue parameters (table 1).

2.3. Phone models

For the exposure of the head models, three phones with different antenna types were used:

- a generic mobile phone equipped with two monopole antennas for two different GSM bands

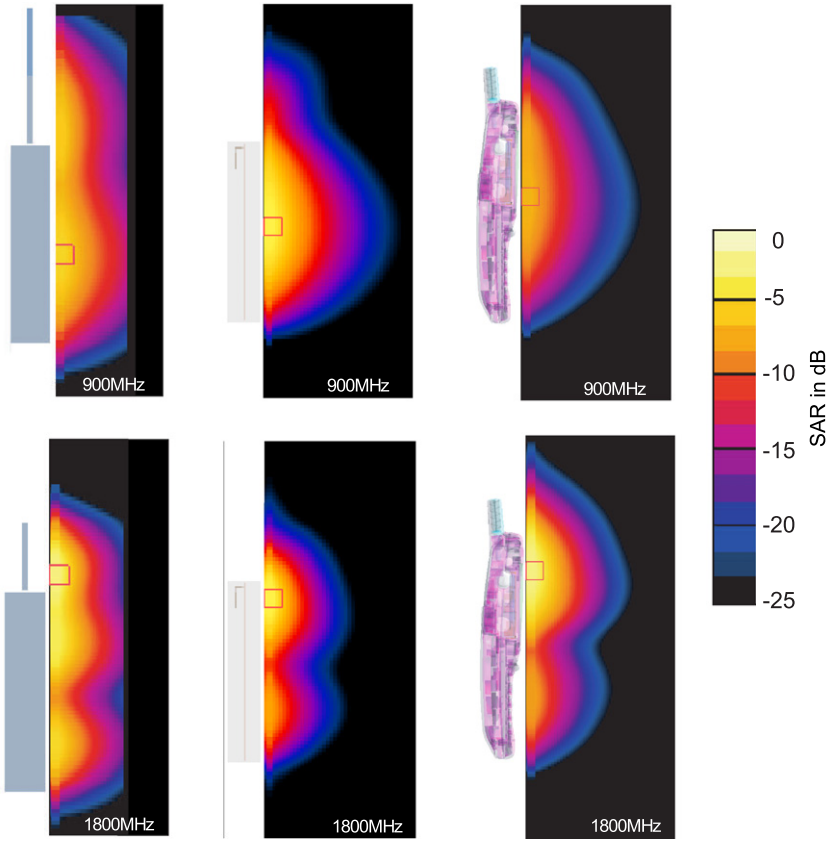

Figure 3. Cross section of the 1 g spatial average SAR distribution in a flat phantom filled with tissue simulant (IEEE 2003) in the plane of the SAR maximum for the three phone models (left: generic monopole, center: generic integrated, right: T250) at a distance of 2 mm and 1 W radiated power (0 dB $\hat{=}$ 25 W kg^{-1}). The red square marks the location of the psSAR.

- a generic mobile phone with an integrated dual band antenna
- a CAD model of the Motorola Timeport T 250 with a helical antenna.

The generic phone with a monopole antenna was originally developed for an interlaboratory comparison of numerical SAR assessment (Beard *et al* 2006). It consists of a perfectly conducting plate enclosed in the center of a dielectric box. Two different antennas for operation in the GSM 900 band and in the GSM 1800 band can be mounted[7]. A detailed characterization of the phone and the validation of the model can be found in Beard *et al* (2006). The generic phone with an integrated dual band antenna was developed as a benchmark for a numerical standard for compliance testing of wireless devices, which is currently under development within a working group of IEEE/ICES TC34 (IEEE 2008). The development and the validation of the numerical model of the Motorola T 250 are described in detail in Chavannes *et al* (2003).

Figure 3 shows the three phone models and their SAR distribution when operated at 900 MHz and 1800 MHz at a distance of 2 mm from a flat phantom filled with tissue simulant.

[7] The phone was originally designed for operation at 835 MHz and 1900 MHz. Its bandwidth is sufficiently large for operation in the GSM 900 and the GSM 1800 bands.

The dielectric parameters of the tissue simulant are $\epsilon_r = 41.5$ and $\sigma = 0.97$ S m^{-1} at 900 MHz and $\epsilon_r = 40.0$ and $\sigma = 1.4$ S m^{-1} at 1800 MHz. For all three devices, the location of the psSAR at 900 MHz is approximately above the center of the case. At 1800 MHz, it is close to the antenna feedpoint at the top of the case.

2.4. Numerical method

For all evaluations, the integrated simulation platform SEMCAD X (Schmid & Partner Engineering AG, Zürich) was used. The radio frequency (RF) solver of SEMCAD X is based on the finite-difference time-domain (FDTD) method (Taflove and Hagness 2000), but has been greatly enhanced with various novel features. The software package was jointly developed with the IT'IS Foundation and has been extensively validated.

For the simulation, a maximum spatial mesh step of 1.5 mm was chosen in the head. In the environment of the phone, i.e. in the regions of maximum exposure, the mesh step was refined to 0.5 mm (generic phones) and 0.15 mm (T250). In free space, the mesh step did not exceed 15 mm. The computational domain was terminated with perfectly matched layers absorbing boundary conditions. A distance of approximately one wavelength was maintained between the head and the phone and the boundaries of the computational domain.

3. Dependence of the exposure on age dependent parameters

3.1. Peak spatial average SAR

For assessment of the impact of the age-dependent changes of the dielectric tissue parameters, the head models of a 3-year-old child, a 6-year-old boy, an 11-year-old girl and a 38-year-old adult (3YC, Thelonious, Billie, Visible Human) were simulated with all four tissue data sets of table 1. The head models were exposed to all three phone models (section 2.3) in the standardized 'touch' and 'tilted' positions (IEEE 2003, IEC 2005)[8]. For all cases, the 10 g psSAR was evaluated in a cubical volume according to the procedure defined in IEEE (2002). The pinnae of the models were excluded from the averaging volume (IEEE 2005).

Figures 4 and 5 show the 10 g psSAR for all models, tissue properties, phones and the two positions at 900 MHz and 1800 MHz. The values were normalized to the 10 g psSAR obtained with the SAM phantom (0 dB, table 2). For most of the configurations, the differences in SAR due to the age-dependent changes of the tissue dielectrics are approximately 0.5 dB at 900 MHz (figure 4) and approximately 1.5 dB or less at 1800 MHz (figure 5) if the anatomical model, phone and exposure position are kept constant. There is, however, no correlation of the age group of the tissue dielectrics with the psSAR. The differences among the head models can reach an order of magnitude of 3 dB for the same configuration (phone, frequency and position). The variations are within the order of magnitude which has been reported for different individuals of the same age group in studies using a large number of head models and configurations, such as (Kainz *et al* 2005). In conclusion, they do not support the assumption of dependence of the psSAR with the age or size of the head model. The differences can rather be attributed to individual anatomical features.

[8] The phone models were positioned against the anatomical head models following the procedure defined in Kainz *et al* (2005).

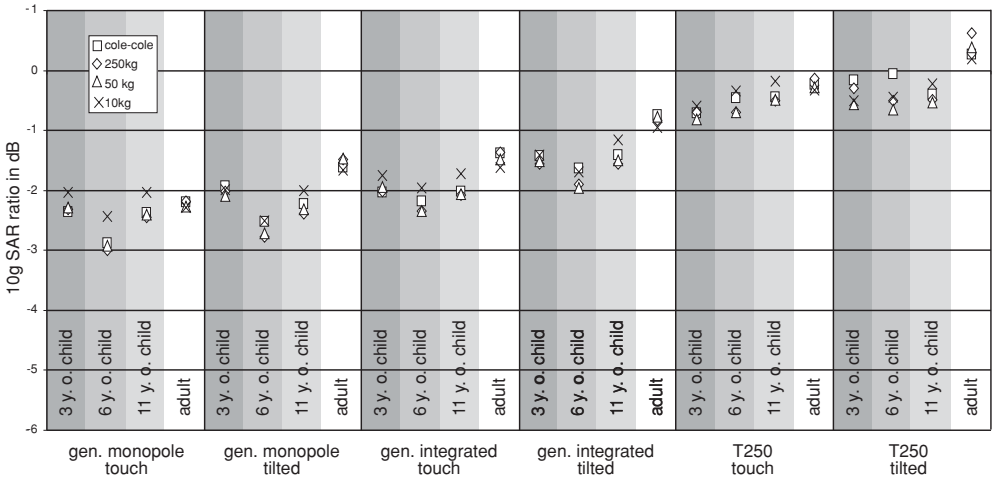

Figure 4. Ratio of the 10 g peak spatial average SAR for exposure of the anatomical models at 900 MHz in comparison to SAM (table 2).

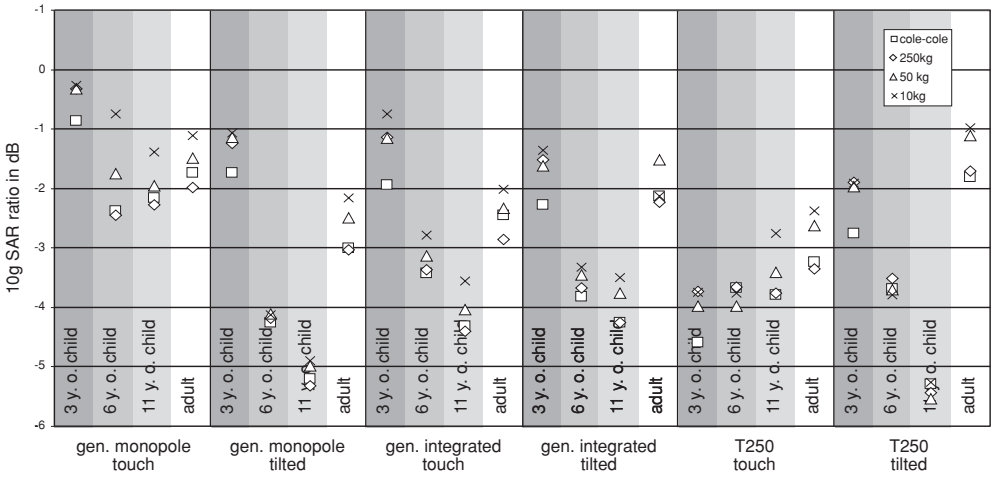

Figure 5. Ratio of the 10 g peak spatial average SAR for exposure of the anatomical models at 1800 MHz in comparison to SAM (table 2).

3.2. Inner head and brain regions

The exposure of the hypothalamus, the pineal gland, the hippocampus and the eye was evaluated for the configurations described in section 3.1. Figure 6 shows the average (arithmetic mean value) of the SAR of these regions of the four age-dependent data sets of tissue dielectrics (section 2.2). The bars indicate the variations due to the age-dependent tissues. The SAR was calculated by dividing the power dissipated in the respective regions by their mass. The reference SAR (0 dB) in figure 6 is again the psSAR of the SAM phantom for the respective configurations (table 2).

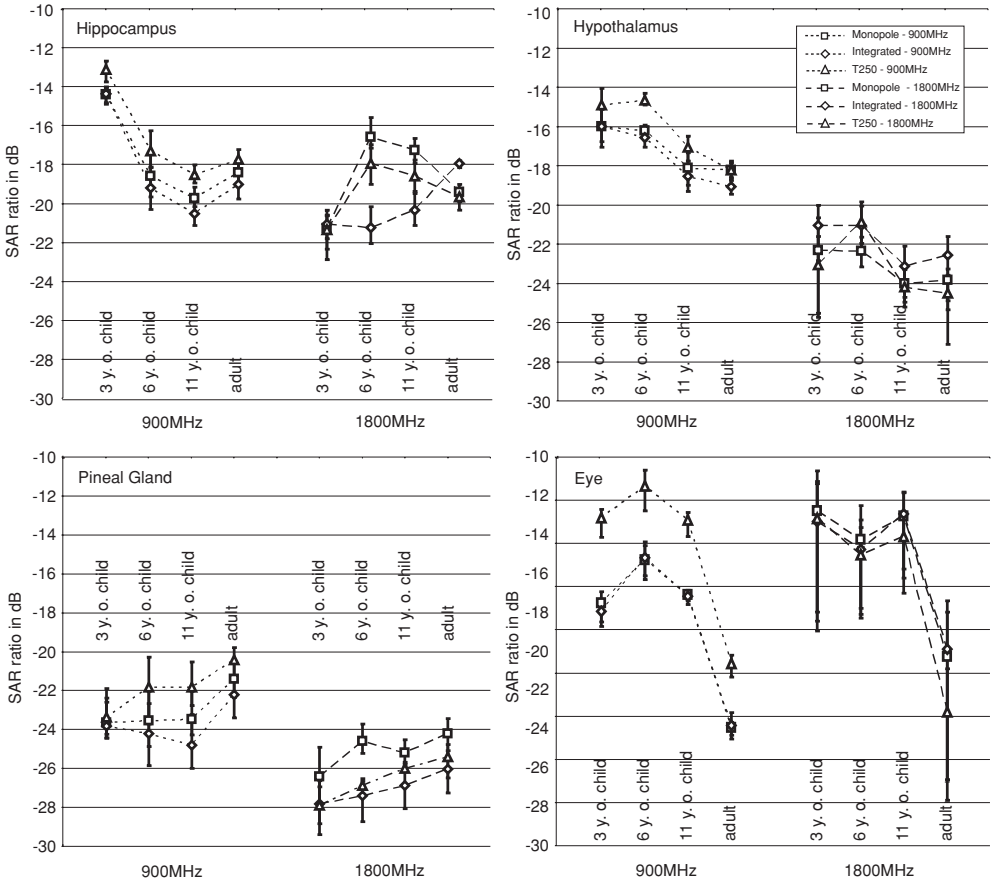

Figure 6. Exposure of the inner regions of the brain and the eye for the three phone models in the *touch* position normalized to the 10 g peak spatial average SAR in SAM (table 2). The bars indicate the variation of the exposure depending on the age group of the dielectric tissue properties.

Table 2. 10 g peak spatial average SAR in W kg^{-1} in the SAM phantom for exposure with the two generic phone models at 1 W radiated power and for the T250 operating in power control level 5 (PCL5, 32 dBm).

	900 MHz		1800 MHz	
	Touch	Tilted	Touch	Tilted
Generic monopole	8.0	4.2	5.3	7.7
Generic integrated	6.7	3.7	5.6	5.0
T250	0.67	0.36	0.56	0.42

Again a general dependency of exposure on the age class of the tissue parameters was not observed. In order to make the graphs of figure 6 more readable, the values of the age-dependent tissue parameter sets are not reported as sets of separate curves. Instead their maxima and minima are indicated by bars as mentioned above. Nevertheless, the exposure of

Table 3. Distances (mm) of the brain and head regions to the entrance of the auditory canal.

	3-year-old child 3YC	6-year-old child Thelonious	11-year-old child Billie	Adult Visible Human
Hypothalamus	79	76	82	92
Hippocampus (left)	84	100	102	100
Hippocampus (right)	63	54	59	69
Eye (left)	117	121	124	147
Eye (right)	90	86	89	103
Pineal Gland	80	80	83	83

the hippocampus, the hypothalamus and the eye shows a reduction that can be correlated with the growth of the proportions of the head with increasing age and can exceed 3 dB.

- The exposure of the hippocampus drops by approximately 5 dB at 900 MHz for the older models in comparison to the three year old (figure 6, top left). At 1800 MHz, the drop of the exposure of the hippocampus within the older models is about 3 dB with the exposure of the three year old and the phone with the integrated antenna as an exception.
- The exposure of the hypothalamus (figure 6, top right) drops by about 3 dB at 900 MHz and about 2 dB at 1800 MHz for increasing age of the models.
- No strong correlation with the age of the head model can be observed for the exposure of the pineal gland (figure 6, bottom left).
- The exposure of the eye drops by 6 dB–10 dB at both 900 MHz and 1800 MHz for the older models (figure 6, bottom right).

Considering the uncertainties due to the differences in the exposure patterns of the phones (figure 3) and the segmentation of the different brain regions, the changes in exposure can be correlated with the distances between the radiation source and the respective brain regions. As a measure for the growth as a function of age, these distances are indicated in table 3 with respect to the auditory canal opening. For the hypothalamus, the hippocampi and the eye, a shorter distance generally corresponds to a higher exposure. The poor correlation of the exposure of the pineal gland with age can also be explained by its position in the head models with respect to the entrance of the auditory canal which is rather constant.

Since the distribution of the current density on the phone can vary significantly depending on frequency, position and individual anatomical properties, the actual distance between the SAR at the exposed brain region and the actual SAR maximum (of all head tissues) will show a certain variation for the different configurations, and in certain cases the entrance of the auditory canal is not the location of the exposure maximum. Nevertheless, the distances as given in table 3 yield the advantage of being an uncomplicated and well-defined indicator of the relative change of the exposed regions during the growth of the head.

3.3. Brain cortex

Section 3.2 has shown that the exposure of inner regions of the head and of the brain can be correlated with their distance from the source of radiation. Moreover, large differences in the exposure of the cortex can occur when the exposed region is close to the surface of the head. Here, the current distribution on the phone can be of particular relevance. In the close near field of a transmitter, the exposure directly depends on the distribution of the RF currents on the conducting parts (Kuster and Balzano 1992). The phone models discussed in section 2.3

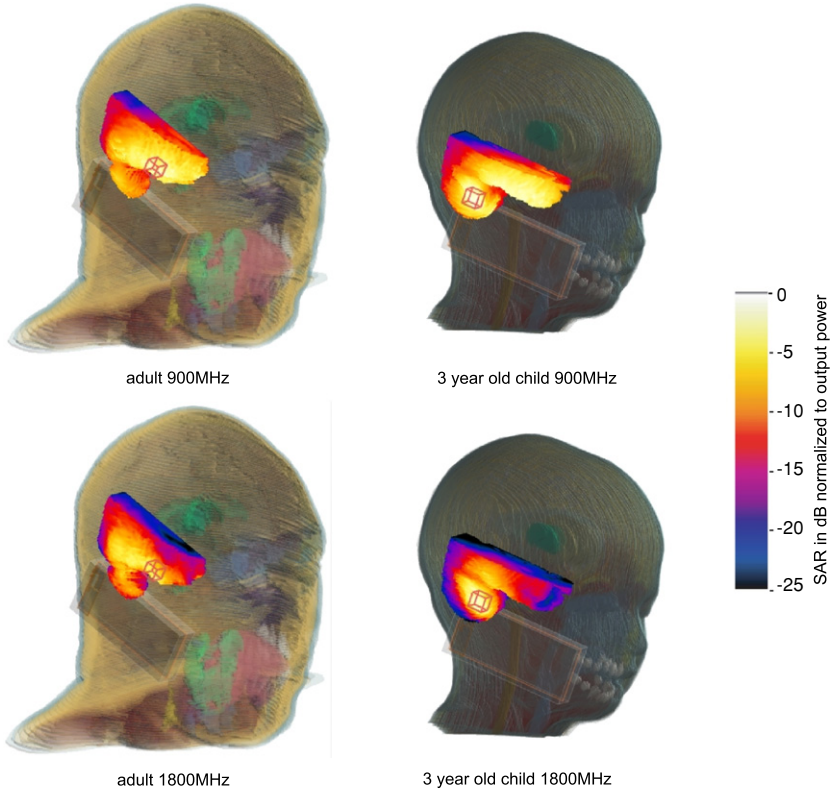

Figure 7. Position of the maximum 1 g peak spatial average SAR (red cube) in the brain of the models of the three year old child and of the 38 year old male adult (Visible Human) when exposed to the generic phone with integrated antenna.

show typical differences in their near-field exposure pattern for the two frequency bands. At 900 MHz the SAR maximum occurs in the center of the case, whereas it is located at the upper edge of the case or at the antenna feedpoint for operation at 1800 MHz (figure 3).

For the comparison of the exposure of the surface regions of the cortex, the models of the 3-year-old child, the 7-year-old child, the 34-year-old male adult and the 38-year-old male adult (3YC, 7YC, Duke and Visible Human) were irradiated with the generic phone with the integrated antenna in 'touch' and 'tilted' positions at 900 MHz and 1800 MHz. Figure 7 shows the SAR distribution on the surface of the brain of the three-year-old child and of the Visible Human. The red cubes indicate the location of the 1 g psSAR in the brains of the models. For the three-year-old child, it is located in the cerebellum at both frequencies (figure 7, right, top and bottom). For the model of the seven-year-old child, the psSAR in the brain also occurs in the cerebellum. For the two adult models (Duke and Visible Human), the 1 g psSAR is located in the temporal lobe, which is shown in figure 7 (left, top and bottom) for the Visible Human model.

At 900 MHz the current maximum is located at the center of the case of the phone (figure 3, top row), and the distance between the current maximum and the location of the psSAR of the two adults and the two children is similar. At 1800 MHz, the current maximum moves to the top of the phone (figure 3, bottom row). Because of the different

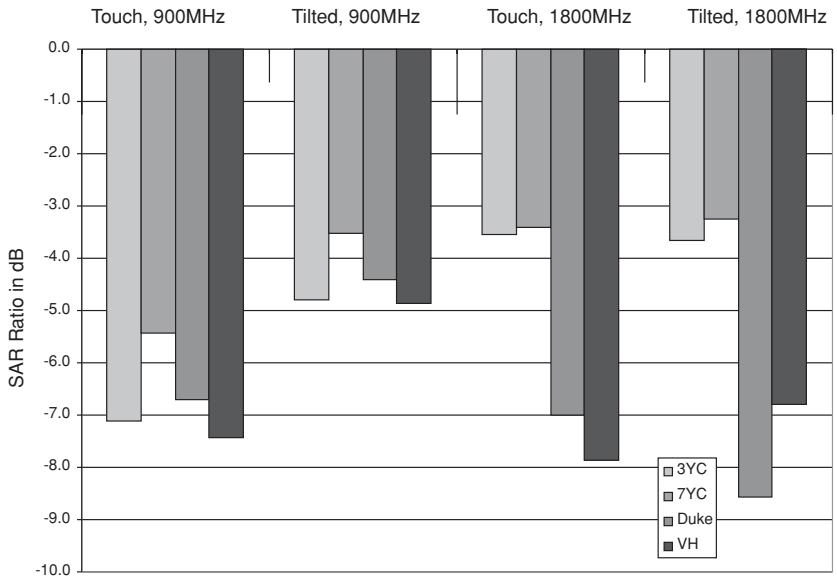

Figure 8. Ratio of the 10 g psSAR in the brain cortices of the models of the three year old child (3YC), the seven year old child (7YC), Duke and the Visible Human (VH) in comparison to 10 g psSAR of the SAM Phantom (table 2) when exposed to the generic telephone with integrated antenna normalized to the output power.

proportions of the heads of adults and children, the distance between the brain and the location of the current maxima on the phones varies significantly at this frequency. For the two adult models, the distance from the phone to the temporal lobe of the adult brain is shorter than the distance to the cerebellum such that the psSAR can also be found there both at 900 MHz and 1800 MHz. The comparison of the 10 g psSAR for these configurations shows that exposure of the brains of the two children and the adults is in the same order of magnitude if the current maximum occurs at the center of the phone case, whereas it can exceed the exposure of the adult brain by more than 4 dB if the current maximum is located at the top of the case (figure 8).

3.4. Bone marrow

Since the distribution of bone marrow in the skull is very complex, large uncertainties during its segmentation are inevitable and may lead to disjoint regions of altering thickness. Therefore, the impact of age-dependent changes of dielectric tissue properties was assessed with the help of a generic layered model: skin (1.5 mm), fat (1.5 mm), bone (1.5 mm), marrow (1.0 mm or 3.0 mm), bone (1.5 mm) and muscle (infinite). The typical range of the thickness of the bone marrow layer in the skull was estimated from the cryosection images of the Visible Human Project (Ackerman 1998). The average thicknesses of the other layers were taken from (Snyder *et al* 1975, Drossos *et al* 2000, Seidenari *et al* 2000). The model was irradiated with dipole antennas operating at 900 MHz and 1800 MHz at a distance of 10 mm. Simplified layered body models for RF exposure assessment were already applied and validated in Drossos *et al* (2000), Christ *et al* (2006a, 2006b). The generic layered model and the dipole antenna (here for 1800 MHz) are shown in figure 9. For near-field-like coupling of the fields into the

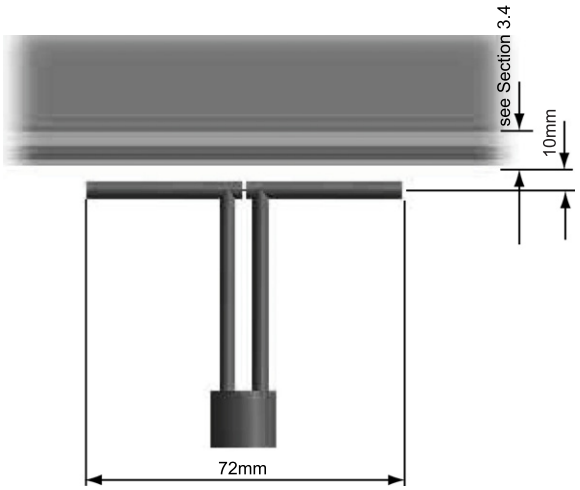

Figure 9. Generic layered body model with dipole antenna with tuning stub (1800 MHz).

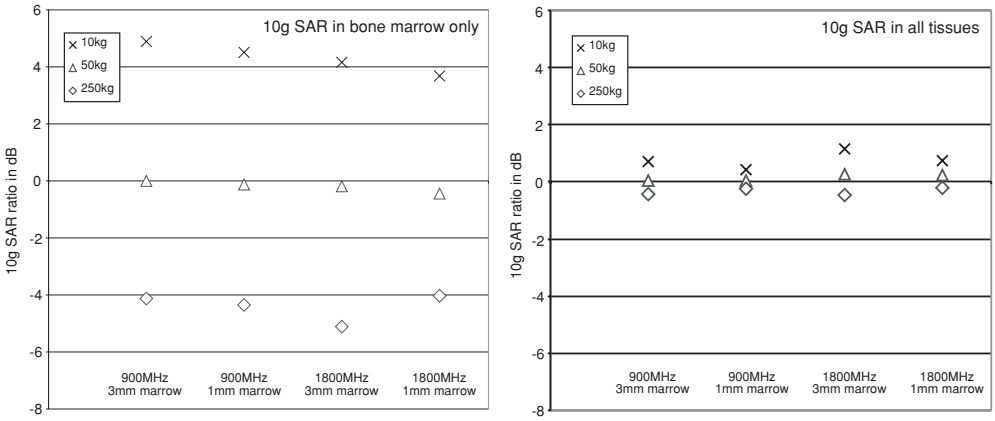

Figure 10. 10 g peak spatial average SAR at 900 MHz and 1800 MHz for age dependence of the dielectric tissue parameters in the layered model (1 mm and 3 mm thickness of the bone marrow layer) averaged over *bone marrow only* and over *all tissues* in comparison to the Cole–Cole model (0 dB).

body, the exposure is governed by the local tissue conductivity, whereas standing wave effects due to reflections at tissue layers with high dielectric contrast can occur for far-field-like coupling.

Figure 10 shows the 10 g psSAR averaged over the bone marrow tissue and compared to the psSAR including all tissues. Absorption in the bone marrow is approximately proportional to its conductivity (table 1) and largely independent of the layer thickness. Therefore, it is clearly age dependent i.e. the exposure of the bone marrow can be 10 dB higher in children than in adults (figure 10, left). It should also be noted that the uncertainty of this ratio is directly proportional to the measurement uncertainty of the dielectric measurements.

4. Summary and conclusions

This study addressed two open questions on the exposure of adults and children to cell phone radiation, namely, (1) the effect of age-dependent tissue parameters for testing compliance with safety standards (IEEE 2003, IEC 2005) and (2) age-dependent differences in the exposure of specific tissues which may be relevant for the interpretation and design of epidemiological studies and volunteer studies.

Regarding the psSAR, which is the relevant quantity for the demonstration of the compliance of mobile phones with safety limits, the conclusions of previous studies (Christ and Kuster 2005) were confirmed (section 3.1):

- Age dependences of dielectric tissue properties do not lead to systematic changes of the psSAR. This is valid for all the configurations analyzed here (phone models, positions, etc).
- The geometrical properties of the head do not have a systematic impact on the psSAR i.e. a correlation between the size of the head and the peak spatial SAR could not be established. Differences are merely due to individual anatomical properties. This is valid for all configurations analyzed here (phone models, positions, etc).
- In all investigated cases, the current methods for compliance testing prove to be conservative.

Major age-dependent changes were observed for the exposure of particular tissues and brain regions. These concern bone marrow as well as regions both inside the brain and at its surface. The findings can be summarized as follows.

- The exposure of regions inside the brains of young children (e.g. hippocampus, hypothalamus, etc) can be higher by more than 2 dB–5 dB in comparison to adults (section 3.2). This should be considered in the design of volunteer studies, e.g., (Huber *et al* 2005, Regel *et al* 2007a, 2007b).
- The exposure of the bone marrow of children can exceed that of adults by about a factor of 10. This is due to the strong decrease in electric conductivity of this tissue with age (section 3.4).
- The exposure of the eyes of children is higher than the exposure of the eyes of adults. Regarding thermal effects, however, this does not represent a problem as the exposure of the eyes by mobile phones is very low i.e. less than −10 dB compared to the psSAR (section 3.2).
- Because of differences in their position with respect to the ear, brain regions close to the surface can exhibit large differences in exposure between adults and children. The cerebellum of children can show a peak spatial average SAR more than 4 dB higher than the local exposure of the cortex of adults. It should be noted that these differences strongly depend on the current distribution of the phone (section 3.3).
- Tissues or regions that have a similar distance to the phone for adults and children, such as the pineal glands, do not experience age-dependent exposure (section 3.3).

In general and on average, children suffer a higher exposure of their brain regions than adults. This higher exposure is due to differences in anatomical proportions. For the exposure of the surface of the brain, the current density distribution or the near field of the cell phone must be regarded. This is of particular importance for the interpretation of epidemiological studies and for research on non-thermal effects. A more detailed and quantitative analysis of the exposure of different brain regions appears necessary and is feasible with the help of additional anatomical models and advanced methods for the evaluation of the brain exposure,

such as the Talairach transformation (Murbach *et al* 2009) that has recently become available for dosimetric simulations.

Acknowledgments

The authors would like to thank Azadeh Peyman and Camelia Gabriel for their advice on the age-dependent changes of tissue dielectrics. This study was generously supported by the German Federal Office for Radiation Protection (Bundesamt für Strahlenschutz).

References

Ackerman M J 1998 The Visible Human Project *Proc. IEEE* **86** 504–11

Beard B *et al* 2006 Comparisons of computed mobile phone induced SAR in the SAM phantom to that in anatomically correct models of the human head *IEEE Trans. Electromagn. Compat.* **48** 397–407

Bit-Babik G, Guy A, Chou C K, Faraone A, Kanda M, Gessner A, Wang J and Fujiwara O 2005 Simulation of exposure and SAR estimation for adult and child heads exposed to radiofrequency energy from portable communication devices *Radiat. Res.* **163** 580–90

CENELEC 2001 Basic standard for the measurement of specific absorption rate related to human exposure to electromagnetic fields from mobile phones (300 MHz–3 GHz) *Standard EN 50361* (Brussels: CENELEC)

Chavannes N, Tay R, Nikoloski N and Kuster N 2003 Suitability of FDTD based TCAD tools for RF design of mobile phones *IEEE Antennas Propag. Mag.* **45** 52–66

Christ A, Chavannes N, Nikoloski N, Gerber H U, Poković K and Kuster N 2005 A numerical and experimental comparison of human head phantoms for compliance testing of mobile telephone equipment *Bioelectromagnetics* **26** 125–37

Christ A and Kuster N 2005 Differences in RF energy absorption in the heads of adults and children *Bioelectromagnetics* **26** S31–44

Christ A, Klingenböck A, Samaras T, Goiceanu C and Kuster N 2006a The dependence of electromagnetic far-field absorption on body tissue composition in the frequency range from 300 MHz to 6 GHz *IEEE Trans. Microw. Theory Tech.* **54** 2188–95

Christ A, Samaras T, Klingenböck A and Kuster N 2006b Characterization of the electromagnetic near-field absorption in layered biological tissue in the frequency range from 30 MHz to 6000 MHz *Phys. Med. Biol.* **51** 4951–66

Christ A, Schmid G, Zefferer M, Überbacher R, Lichtsteiner M, Neufeld E, Cecil S and Kuster N 2008 Numerische Bestimmung der Spezifischen Absorptionsrate bei Ganzkörperexposition von Kindern: part 2. Zwischenbericht *Technical Report* IT'IS Foundation, ETH Zürich, Zeughausstr. 43, 8004 Zürich, Switzerland http://www.emf-forschungsprogramm.de/akt_emf_forschung.html/dosi_HF_003.html (in German)

Christ A *et al* 2010 The Virtual Family—development of anatomical CAD models of two adults and two children for dosimetric simulations *Phys. Med. Biol.* **55** N23–38

Drossos A, Santomaa V and Kuster N 2000 The dependence of electromagnetic energy absorption upon human head tissue composition in the frequency range of 300–3000 MHz *IEEE Trans. Microw. Theory Tech.* **48** 1988–95

Gabriel C 2005 Dielectric properties of biological tissue: variation with age *Biolectromagnetics* **26** S12–8

Gabriel S, Lau R W and Gabriel C 1996a The dielectric properties of biological tissues: II. Measurements in the frequency range 10 Hz to 20 GHz *Phys. Med. Biol.* **41** 2251–69

Gabriel S, Lau R W and Gabriel C 1996b The dielectric properties of biological tissues: III. Parametric models for the dielectric spectrum of tissues *Phys. Med. Biol.* **41** 2271–93

Hand J W 2008 Modelling the interaction of electromagnetic fields (10 MHz–10 GHz) with the human body: methods and applications *Phys. Med. Biol.* **53** R243–86

Huber R, Treyer V, Schuderer J, Berthold T, Buck A, Kuster N, Landolt H P and Achermann P 2005 Exposure to pulse-modulated radio frequency electromagnetic fields affects regional cerebral blood flow *Eur. J. Neurosci.* **21** 1000–6

Huss A, Spoerri A, Egger M and Röösli M 2009 Residence near power lines and mortality from neurodegenerative diseases: longitudinal study of the Swiss population *Am. J. Epidemiol.* **169** 167

ICNIRP 1998 Guidelines for limiting exposure to time-varying electric, magnetic and electromagnetic fields (up to 300 GHz) *Health Phys.* **74** 494–522

IEC 2005 Human exposure to radio frequency fields from handheld and body-mounted wireless communication devices—Human models, instrumentation and procedures: part 1. Procedure to determine the specific absorption

rate (SAR) for handheld devices used in close proximity to the ear (frequency range of 300 MHz to 3 GHz *IEC 62 209* (Geneva: IEC)

IEEE 2002 Recommended practice for measurements and computations of radio frequency electromagnetic fields with respect to human exposure to such fields, 100 kHz—300 GHz *IEEE Std C95.3* (New York: IEEE)

IEEE 2003 Recommended practice for determining the spatial-peak specific absorption rate (SAR) in the human body due to wireless communications devices: measurement techniques *IEEE 1528* (New York: IEEE)

IEEE 2005 IEEE standard for safety levels with respect to human exposure to radio frequency electromagnetic fields, 3 kHz to 300 GHz *IEEE Std C95.1-2005* (New York: IEEE)

IEEE 2008 Draft recommended practice for determining the spatial-peak specific absorption rate (SAR) in the human body due to wireless communications devices, 30 MHz–6 GHz: general requirements for using the finite difference time domain (FDTD) method for SAR calculations *Technical Report IEEE 1528.1 D1.0*

IFAC 2007 Internet resource for the calculation of the dielectric properties of body tissues in the frequency range 10 Hz–100 GHz http://niremf.ifac.cnr.it/tissprop

Kainz W, Christ A, Kellom T, Seidman S, Nikoloski N, Beard B and Kuster N 2005 Dosimetric comparison of the specific anthropomorphic mannequin (SAM) to 14 anatomical head models using a novel definition for the mobile phone positioning *Phys. Med. Biol.* **50** 3423–45

Kheifets L, Repacholi M, Saunders R and van Deventer E 2005 The sensitivity of children to electromagnetic fields *Pediatrics* **116** e303–e313

Khurana V, Moulder J and Orton C 2008 There is currently enough evidence and technology available to warrant taking immediate steps to reduce exposure of consumers to cell-phone-related electromagnetic radiation *Med. Phys.* **35** 5203

Khurana V, Teo C, Kundi M, Hardell L and Carlberg M 2009 Cell phones and brain tumors: a review including the long-term epidemiologic data *Surg. Neurol.* **72** 205–214

Kundi M 2009 The controversy about a possible relationship between mobile phone use and cancer *Environ. Health Perspect.* **117** 316–24

Kuster N and Balzano Q 1992 Energy absorption mechanism by biological bodies in the near field of dipole antennas above 300 MHz *IEEE Trans. Veh. Technol.* **41** 17–23

Martens L 2005 Electromagnetic safety of children using wireless phones: a literature review *Bioelectromagnetics* **7** S133–7

Murbach M, Christopoulou M, Christ A, Crespo-Valero P, Zefferer M, Kühn S, Achermann P and Kuster N 2009 System to study CNS responses of ELF modulation and cortex versus subcortical RF exposures *Proc. of the 31st Ann. Meeting of the Bioelectromagnetics Society (June 14th–19th, Davos, Switzerland 2009)*

Pethig R 1987 Dielectric properties of body tissues *Clin. Phys. Physiol. Meas.* **8** 5–12

Peyman A, Rezazadeh A A and Gabriel C 2001 Changes in the dielectric properties of rat tissue as a function of age at microwave frequencies *Phys. Med. Biol.* **46** 1617–29

Peyman A, Gabriel C, Grant E H, Vermeeren G and Martens L 2009 Variation of the dielectric properties of tissues with age: the effect on the values of SAR in children when exposed to walkie-talkie devices *Phys. Med. Biol.* **54** 227–41

Regel S J, Gottselig J M, Schuderer J, Tinguely G, Rétey J V, Kuster N, Landolt H P and Achermann P 2007a Pulsed radio frequency radiation affects cognitive performance and the waking electroencephalogram *Neuroreport* **18** 803–7

Regel S J, Tinguely G, Schuderer J, Adam M, Kuster N, Landolt H P and Achermann P 2007b Pulsed radio-frequency electromagnetic fields: dose-dependent effects on sleep, the sleep EEG and cognitive performance *J. Sleep Res.* **16** 253–8

Schmid G and Überbacher R 2005 Age dependence of dielectric properties of bovine brain and ocular tissues in the frequency range of 400 MHz to 18 GHz *Phys. Med. Biol.* **50** 4711–20

Schönborn F, Burkhardt M and Kuster N 1998 Differences in energy absorption between heads of adults and children in the near field of sources *Health Phys.* **74** 160–8

Schüz J, Waldemar G, Olsen J and Johansen C 2009 Risks for central nervous system diseases among mobile phone subscribers: a Danish retrospective cohort study *PLoS ONE* **4** e4389

Seidenari S, Giusti G, Bertoni L and Magnoni C 2000 Thickness and echogenicity of the skin in chrildren as assesseed by 20 MHz ultrasound *Dermatology* **201** 218–22

Snyder W S, Cook M J, Nasset E S, Karhausen L R, Howells G P and Tipton I H 1975 *Report of the Task Group on Reference Man ICRP-23* 1st edn (Oxford: Elsevier Science)

Stauffer P R, Rossetto F, Prakash M, Neuman D G and Lee T 2003 Phantom and animal tissues for modelling the electrical properties of human liver *Int. J. Hyperth.* **19** 89–101

Taflove A and Hagness S C 2000 *Computational Electromagnetics: The Finite-Difference Time-Domain Method* 2nd edn (Boston, MA: Artech House Publishers)

Thurai M, Goodridge V D, Sheppard R J and Grant E H 1984 Variation with age of the dielctric properties of mouse brain cerebrum *Phys. Med. Biol.* **29** 1133–6

Thurai M, Steel M C, Shepard R J and Grant E H 1985 Dielectric properties of developing rabbit brain at 37 degrees *Bioelectromagnetics* **6** 235–42

Wang J, Fujiwara O and Watanabe S 2006 Approximation of aging effect on dielectric tissue properties for SAR assessment of mobile telephones *IEEE Trans. Electromagn. Compat.* **48** 408–13

Wiart J, Hadjem A, Gadi N, Bloch I, Wong M F, Pradier A, Lautru D, Hanna V F and Dale C 2005 Modeling of RF head exposure in children *Bioelectromagnetics* **26** S19–S30

Wiart J, Hadjem A, Wong M and Bloch I 2008 Analysis of RF exposure in the head tissues of children and adults *Phys. Med. Biol.* **53** 3681